Molecular Biology of the Cell
Vol. 20, 1903–1915, April 1, 2009

Cooperative Assembly and Misfolding of CFTR Domains In Vivo

Kai Du and Gergely L. Lukacs

Department of Physiology, McGill University, Montreal, Quebec, Canada H3G 1Y6

Submitted September 18, 2008; Revised January 7, 2009; Accepted January 22, 2009
Monitoring Editor: Reid Gilmore

The cystic fibrosis transmembrane conductance regulator (CFTR) architecture consists of two membrane spanning domains (MSD1 and -2), two nucleotide binding domains (NBD1 and -2), and a regulatory (R) domain. Several point mutations lead to the channel misprocessing, with limited structural perturbation of the mutant domain. To gain more insight into the basis of CFTR folding defect, the contribution of domain-wise and cooperative domain folding was assessed by determining 1) the minimal domain combination that is recognized as native and can efficiently escape the endoplasmic reticulum (ER) retention and 2) the impact of mutation on the conformational coupling among domains. One-, two-, three-, and most of the four-domain assemblies were retained at the ER. Solubilization mutations, however, rescued the NBD1 processing defect conceivably by thermodynamic stabilization. The smallest folding unit that traversed the secretory pathway was composed of MSD1-NBD1-R-MSD2 as a linear or split polypeptide. Cystic fibrosis-causing missense mutations in the MSD1, NBD1, MSD2, and NBD2 caused conformational defect in multiple domains. We propose that cooperative posttranslational folding is required for domain stabilization and provides a plausible explanation for the global misfolding caused by point mutations dispersed along the full-length CFTR.

INTRODUCTION

Cystic fibrosis (CF), the most common genetic disease in the Caucasian population, is caused by the impaired functional expression of cystic fibrosis transmembrane conductance regulator (CFTR), a cAMP-regulated chloride channel that belongs to the ATP-binding cassette (ABC) transporter superfamily (Riordan *et al*., 1989). The distinct domain organization of CFTR is hallmarked by the acquisition of a regulatory (R) domain, connecting the two halves of the channel, each containing a membrane spanning domain (MSD) and a nucleotide binding domain (NBD) (MSD1-NBD1 and MSD2-NBD2) (Riordan *et al*., 1989; Sheppard and Welsh, 1999). The regulatory (R) domain is largely unstructured (Ostedgaard *et al*., 2000a), and, in coordination with the NBDs, regulates the gating of CFTR (Riordan, 2005). After cotranslational insertion into the ER, the nascent CFTR chain undergoes inefficient conformational maturation, mediated by molecular chaperones that require cytoplasmic ATP (Lukacs *et al*., 1994; Meacham *et al*., 1999; Oberdorf *et al*., 2005). Multiple quality control checkpoints ensure that native channels enter the secretory pathway via COPII transport vesicles (Wang *et al*., 2004; Wang *et al*., 2006; Younger *et al*., 2006), whereas partially folded molecules are eliminated by the endoplasmic reticulum (ER)-associated degradation (ERAD), using the ubiquitin-proteasome system (Kopito, 1999; Nakatsukasa and Brodsky, 2008).

CFTR folding intermediates and off-pathway conformers are recognized by molecular chaperones, presumably by their association with exposed hydrophobic segments in the cytosol or the ER lumen (Laney and Hochstrasser, 1999; Meacham *et al*., 1999, 2001; Youker *et al*., 2004; Young *et al*., 2004; Nakatsukasa and Brodsky, 2008). CFTR domain assembly may also confer quality control checkpoints by regulating the accessibility of linear ER export and retention signals in analogy with oligomerization of multisubunit channels (Ellgaard and Helenius, 2003). The arginine-based ER sorting signal was first described as a quality control check point for the K_{ATP} channel assembly (Zerangue *et al*., 1999). Two Arg-X-Arg (RXR) motifs in the MSD1 and NBD1 seem to play a role in the ER retention of misfolded CFTR as well (Chang *et al*., 1999). Masking of the diacidic ER export motif was also proposed as a complementary mechanism for the ER retention of the nonnative CFTR (Wang *et al*., 2004).

Deletion of phenylalanine 508 (ΔF508 CFTR) in the NBD1, manifests in virtually complete ER retention and degradation of the channel by the ubiquitin proteasome system (Kopito, 1999; Riordan, 2005). The structural consequence of the ΔF508 mutation as a recognition signal for the cellular quality control mechanisms has received much attention (Riordan, 2005). At the domain level, the x-ray crystal structure revealed marginal differences between the wild-type (wt) and ΔF508 NBD1 overall fold (Lewis *et al*., 2005; Thibodeau *et al*., 2005). Amino acid substitutions at the 508 position were permissive for the NBD1 folding, whereas deletion of F508 decreased the domain folding yield without influencing its stability (Lewis *et al*., 2005; Thibodeau *et al*., 2005). In contrast, most amino acid substitutions were nonpermissive for the in vivo biogenesis of CFTR (Du *et al*., 2005; Thibodeau *et al*., 2005). ΔF508 also increased the MSD1 and NBD2 protease susceptibility with modest, but detectable effect on the NBD1 (Du *et al*., 2005; Cui *et al*., 2007). These observations, together with the destabilization of the MSD1-NBD1-R by the ΔF508, have led to the hypothesis that the F508 residue is indispensable for the MSD1-NBD1-R (Rosser *et al*., 2008) and MSD1/NBD2 conformational mat-

This article was published online ahead of print in *MBC in Press* (http://www.molbiolcell.org/cgi/doi/10.1091/mbc.E08–09–0950) on January 28, 2009.

Address correspondence to: Gergely L. Lukacs (gergely.lukacs@mcgill.ca).

uration, although the precise mechanism of misfolding remained incompletely understood (Riordan, 2008).

Although individual CFTR domains are likely to attain loosely folded, near-native conformation cotranslationally to minimize intra- and intermolecular aggregation (Sadlish and Skach, 2004; Kleizen *et al*., 2005), the compactly folded channel seems to assemble posttranslationally (Du *et al*., 2005). This conclusion is consistent with the prolonged association of chaperones with the nascent CFTR chain (Meacham *et al*., 1999, 2001) and the delayed, posttranslational appearance of protease resistant, mature CFTR and NBD2 (Du *et al*., 2005). Numerous interactions among the major domains (e.g., NBD1-NBD2, MSD1-MSD2, NBDs-MSDs, and R-NBD1), as well as the N- and C-terminal tails have been identified in the native CFTR, by using recombinant domains (Riordan, 2005). These interactions may be involved in domain folding, assembly and stability, or in a combination of these factors.

To better understand the molecular basis of CFTR domain assembly and misfolding, we determined the in vivo folding capacity of wild type and mutant domains individually and in combinations. We report that single domains and most of the domain combinations are largely recognized as nonnative conformers by the ER quality control in vivo, with the caveat that the NBD1 processing defect was rescued by mutations that stabilized the domain in vitro. Point mutations in the MSD1, NBD1, MSD2 or NBD2 led to the cooperative, global misfolding of multiple domains. Collectively, these and other results suggest that interdependent domain assembly represents a critical step for the channel biogenesis and offers a plausible explanation for the cooperative misfolding and ER retention, caused by numerous CF-associated mutations dispersed along the full-length CFTR. A preliminary account of this study has been published as an abstract (Du and Lukacs, 2007).

MATERIALS AND METHODS

Cell Lines

Baby hamster kidney (BHK) cells, stably expressing the wt and mutant (G91R, L346P, L1093P, N1303K, ΔF508, 4D, 1218X, 1158X, and 823X) CFTR with three tandem hemagglutinin (HA)-epitope (3HA) inserted into the fourth extracellular loop, were isolated and maintained as described previously (Sharma *et al*., 2004; Du *et al*., 2005). At least 50 individual clones were combined after antibiotic selection and expanded for subsequent experiments. CFTR fragments were transiently expressed in BHK and COS7 cells using the FuGENE 6 (Roche Applied Science, Indianapolis, IN). BHK and COS7 cells were grown in DMEM/F-12 (5% fetal bovine serum [FBS]) and in DMEM (10% of FBS), respectively, at 37°C under 5% CO_2.

Antibodies and Reagents

Antibodies (Abs) were obtained from the following sources. Monoclonal anti-CFTR Ab L12B4 (recognizing 386-412 residues of the NBD1) and M3A7 (recognizing 1365-1395 residues at the C terminus of the NBD2) (Millipore Bioscience Research Reagents, Temecula, CA); and MM13-4 mouse monoclonal anti-CFTR Ab (specific to the N-terminal 25-36 residues) (Millipore, Billerica, MA). Rabbit anti-NBD1-R (#4562) serum was kindly provided by Dr. D. Badwell (University of Birmingham, Burmingham, AL). A rabbit serum was raised against a glutathione transferase (GST) fusion protein of the C-terminal 80 residues of CFTR. The 660 anti-CFTR Ab recognizes the NBD1 (Cui *et al*., 2007) and was kindly provided by Dr. J. Riordan (University of North Carolina, Chapel Hill, NC). Mouse monoclonal anti-HA Ab was from Covance Innovative Antibodies, (Berkeley, CA) anti-CD4 Ab (OKT4) was from American Type Culture Collection (Manassas, VA), rabbit anti-CD4 Ab was from Santa Cruz Biotechnology (Santa Cruz, CA), and anti-CD74 (invariant chain) Ab was from BD Biosciences (San Jose, CA). Endoglycosidase H (Endo H) and peptide-N^{-}-(*N*-acetyl-β-glucosaminyl)asparagine amidase (PNGase F) were purchased from New England Biolabs (Ispwich, MA). *N*-Tosyl-L-phenylalanine chloromethyl ketone-treated trypsin was purchased from Worthington Biochemicals (Freehold, NJ), and other chemicals were obtained from Sigma-Aldrich (St. Louis, MO) at highest grade available.

CFTR Expression Constructs

N- and C-Terminal domain deletions of CFTR were accomplished by introducing a Kozak consensus initiation site and a stop codon, respectively, into the desired construct by polymerase chain reaction (PCR) mutagenesis by using the CFTR-3HA cDNA as template. CFTR cDNA fragments were subcloned into the pNut expression vector. The enhanced green fluorescent protein (EGFP)-CFTR fusions were obtained from the pcDNA3-EGFP-CFTR plasmid, incorporating a 16-residue linker between C terminus of the EGFP and CFTR (Benharouga *et al*., 2003). To disrupt the NBD1 hydrophobic core, 4D mutations were engineered in two steps. After the insertion of the 2D (I601D/L602D) mutations, the L570D/L571D mutations were introduced into the 2D CFTR-3HA by PCR mutagenesis. The cytosolic domains (NBD1, NBD1-R, and NBD2) and their mutant counterparts (ΔF508, 4D, and N1303K) were PCR amplified with specified amino acid boundaries (Supplemental Table S1) flanked with the XmaI/XbaI sites and fused in frame to the C terminus of the transmembrane segment of the CD4T (CD4T-N1, CD4T-N1R, CD4T-N2, etc.; Supplemental Table S1). The R domain was fused to the truncated Ii chain (IiT), lacking the N-terminal 33 amino acid residues, as well as its trimerization motif. Trimerization of the IiT was disrupted by the Q63A/T65A/T66A mutations (Ashman and Miller, 1999). The domain boundaries of the constructs are summarized in Supplemental Table S1. All constructs were sequence verified.

Microsome Preparation, Limited Proteolysis, and Immunoblotting

Microsomes were prepared by nitrogen cavitation and differential centrifugation and subjected to limited proteolysis as described previously (Zhang *et al*., 1998; Du *et al*., 2005). Immunoblots, with multiple exposures, were quantified using DuoScan transparency scanner and NIH Image 6.1 software (http://rsb.info.nih.gov/nih-image/). To accumulate the folded, core-glycosylated wt CFTR, BHK cells were treated with 10 μg/ml brefeldin A (BFA) for 24 h before the isolation of microsomes.

Endoglycosidase Treatment

To discriminate between core-glycosylated and complex-glycosylated forms of CFTR fragments, detergent solubilized proteins (100 μg of protein) were denatured in 0.5% SDS and 1% β-mercaptoethanal at 30°C for 10 min. Then, polypeptides were incubated with 500 U of Endo H (in 50 mM sodium citrate, pH 5.5) or with 500 U of PNGase F (in 50 mM sodium phosphate, pH 7.5, 1% of NP-40) at 30°C for 3 h.

Immunoprecipitation, Metabolic Pulse-Chase Labeling, and Folding Kinetics of CFTR

Metabolic labeling and immunoprecipitation were performed essentially as described previously (Du *et al*., 2005). Monolayer cells were pulse-labeled for 8–15 min and chased at the indicated temperature. Membrane proteins were solubilized in 1 ml of radioimmunoprecipitation assay buffer (150 mM NaCl, 20 mM Tris-HCl, 1% Triton X-100, 0.1% SDS, and 0.5% sodium deoxycholate, pH 8.0) supplemented with protease inhibitors (10 μg/ml leupeptin and pepstatin, 0.5 mM phenylmethylsulfonyl fluoride, and 10 mM iodoacetamide). Immunoprecipitates, obtained with anti-HA, or M3A7 and L12B4 anti-CFTR monoclonal Ab, were analyzed by SDS-polyacrylamide gel electrophoresis and fluorography. The radioactivity was quantified using a PhosphorImager (Molecular Dynamics, Sunnyvale CA) with the ImageQuant software (Molecular Dynamics) (Lukacs *et al*., 1994). CFTR fragments were coprecipitated from transiently transfected COS7 or BHK cells after solubilization in phosphate-buffered saline (PBS) containing 0.2% NP-40 and protease inhibitors.

To monitor the wt and 1218X CFTR folding in the ER, newly synthesized channels were radioactively labeled for 8 min in the presence of BFA essentially as described previously (Du *et al*., 2005). After 0- to 60-min chase in BFA, folding was terminated by ATP-depletion and cells were kept in the same medium for 2–3 h to ensure the core-glycosylated, nonnative conformer complete elimination. This allowed the quantification of folded CFTR.

Determination of the cAMP-stimulated Iodide Conductance of the Plasma Membrane

The plasma membrane cAMP-dependent halide conductance of transfected BHK cells was determined with the iodide efflux assay as described previously (Du *et al*., 2005).

Immunofluorescence Microscopy

Colocalization of full-length or truncated CFTR with the ER or cell surface markers was analyzed in COS7 and BHK cells by laser confocal fluorescence microscopy essentially as described previously (Barriere *et al*., 2007). Plasma membrane accumulation was documented by coimmunostaining of the 3HA-CFTR fragment with Alexa594-conjugated wheat germ agglutinin (WGA) in 4% paraformaldehyde-fixed, nonpermealized cells. Control experiments verified that fixation preserved the integrity of the plasma membrane. Single

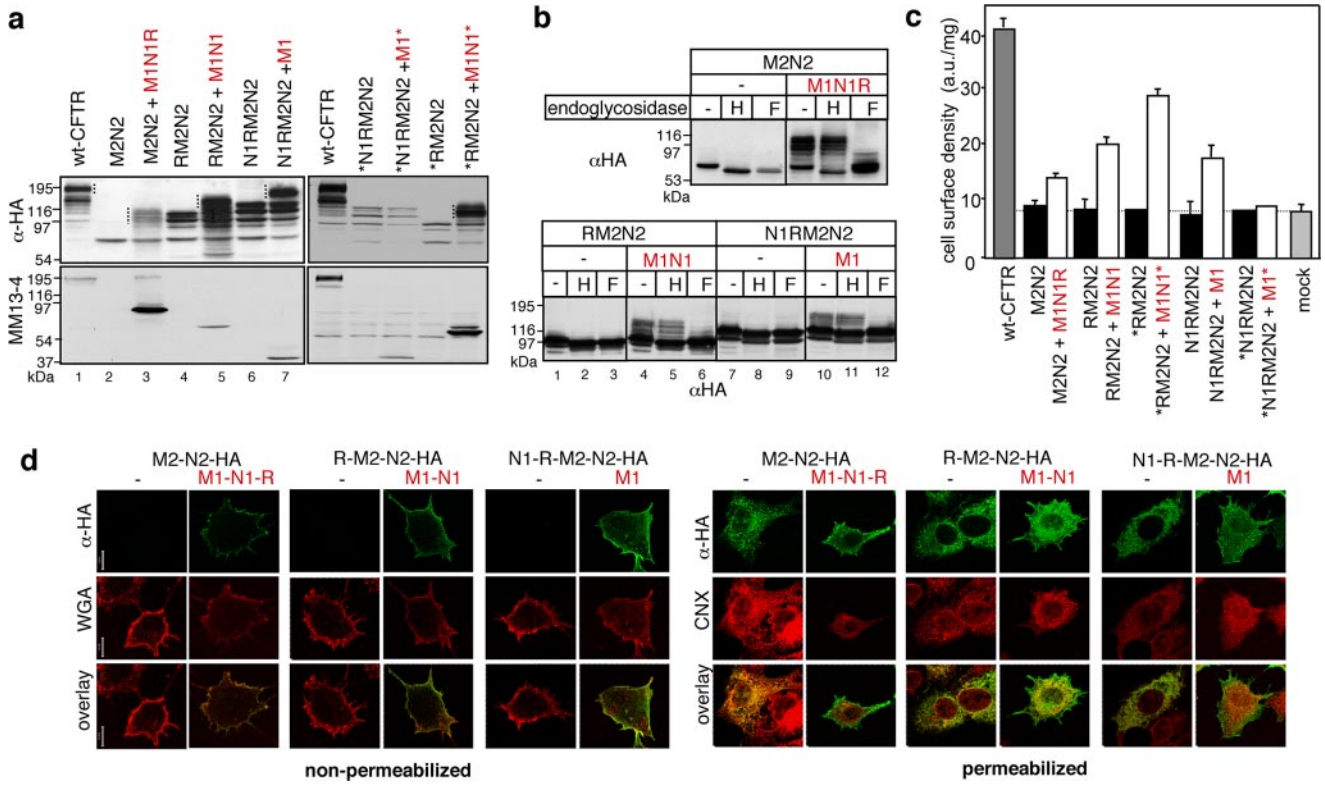

Figure 1. Biosynthetic processing of split CFTR in mammalian cells. (a) The indicated C-terminal CFTR domains (M2N2, RM2N2, N1RM2N2, *RM2N2, and *N1RM2N2) in the absence or presence of complementing N-terminal fragments (M1N1R, M1N1, M1, M1N1*, and M1*, respectively) were transiently expressed in COS7 cells and analyzed by immunoblotting using anti-HA and MM13-4 Abs, recognizing the 3HA epitope in the MSD2 (M2) and the N-terminal tail of the MSD1, respectively. Dotted lines indicate the complex-glycosylated bands, based on endoglycosidase analysis shown in b. (b) Endoglycosidase sensitivity of M2-containing CFTR fragments. Cell lysates, obtained from COS7 cells expressing the indicated CFTR fragments were incubated with endoglycosidase-H (H) or PNGase F (F) and analyzed by immunoblotting with anti-HA antibody. (c) Cell surface density of the CFTR-3HA C-terminal fragments was measured by the immunoperoxidase assay using anti-HA Ab as described in c. Ab binding was normalized for cellular protein (means ± SEM, n = 2–4). (d) Processing of the C-terminal CFTR fragments was monitored by immunostaining in nonpermeabilized (left) and permeabilized (right) cells in the absence or presence of the complementing N-terminal half. The plasma membrane and the ER were visualized by Alexa594-conjugated WGA and CNX staining, respectively. Bar, 10 μm.

optical sections were obtained on an LSM 510 fluorescence laser confocal microscope (Carl Zeiss, Jena, Germany) (Barriere *et al.*, 2007).

Cell Surface Density Measurements of CFTR Variants and Domain Chimeras

The cell surface density of CD4 and Ii chimeras as well as CFTR variants was determined after the binding of mouse monoclonal anti-CD4 (OKT4), anti-Ii or anti-HA primary Ab (0°C for 1 h), and horseradish-peroxidase (HRP)-conjugated goat anti-mouse secondary Ab (0°C for 1 h; GE Healthcare, Chalfont St. Giles, Buckinghamshire, United Kingdom) in PBS supplemented with 1 mM $MgCl_2$, 0.1 mM $CaCl_2$, and 0.5% bovine serum albumin as described previously (Sharma *et al.*, 2004; Barriere *et al.*, 2007). The HRP activity was measured with Amplex Red (Invitrogen, Carlsbad, CA) at 4°C, and the fluorescence intensity was determined by a POLARstar (BMG Labtech, Durham, NC) plate-reader. Nonspecific binding of the Abs was measured in mock-transfected cells. Each experiment was repeated at least two to three times and performed in triplicate.

RESULTS

Domain Boundaries of CFTR

The ambiguity of domain definition according to functional, structural, and homology-based criteria prompted us to use both functional and structural boundaries that have been optimized to reconstitute the ion channel activity of split CFTR in *Xenopus* oocyte (Chan *et al.*, 2000) and to crystallize the NBD1 (Lewis *et al.*, 2005), respectively. The domain abbreviations (MSD1, M1; NBD1, N1; MSD2, M2; and NBD2, N2) and boundaries with predicted molecular masses are summarized in Supplemental Table S1. Domain boundaries corresponding to the NBD1 crystal structure are indicated by an asterisk (*).

The biosynthetic processing of CFTR severed at the MSD1/NBD1, NBD1/R, or R/MSD2 domain interface (Supplemental Figure S1a) was determined by biochemical, morphological, and cell surface antibody binding assays in transiently transfected COS7 and BHK cells. Processing of the C-terminal domain combinations (M2-N2, R-M2-N2, N1-R-M2-N2, *R-M2-N2, and *N1-R-M2-N2), containing the MSD2 was indicated by decreased electrophoretic mobility and resistance to Endo H upon conversion of the high-mannose to complex-type N-glycans in the Golgi complex (Figure 1, a and b). Biosynthetic processing occurred exclusively in the presence of the complementary NH_2-terminal segment (M1-N1-R, M1-N1, M1-N1* and M1, respectively) (Figure 1, a and b). The lack of complementation with M1* and *N1-R-M2-N2 fragments is not fully understood but is conceivably due to the destabilization of the MSD1.

Plasma membrane accumulation of the C-terminal fragments, harboring the extracellular 3HA-tag, was verified by the anti-HA Ab binding assay (Figure 1c). Remarkably, the

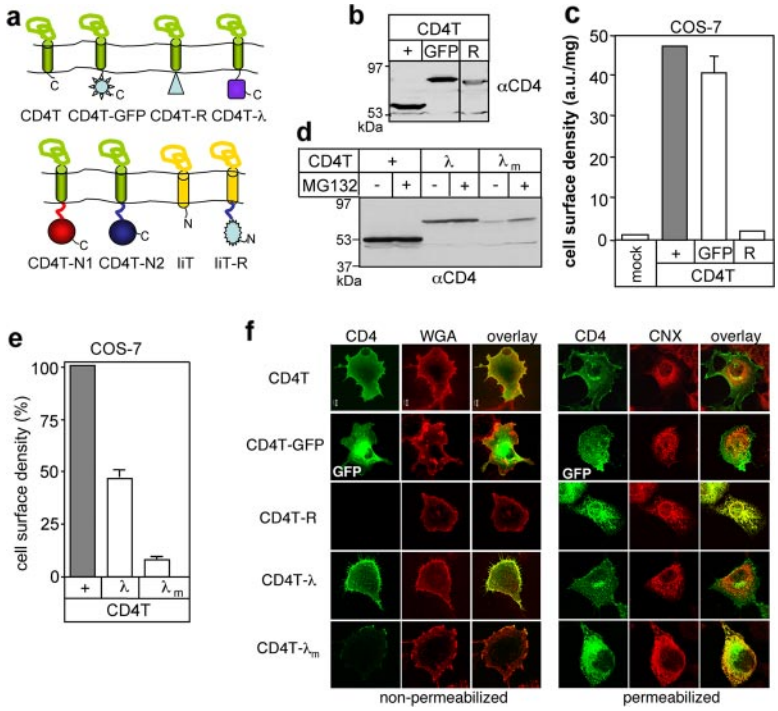

Figure 2. Cell-based assay to monitor the conformation of membrane tethered soluble CFTR domains. (a) Schematic structure of chimeras consisting of the truncated CD4 (CD4T) or invariant chain (IiT). CD4T-λ and CD4T-λ_m contain the wt or the mutant (L57C/L69G) λ repressor, respectively. The CD4T-GFP, CD4T-N1, CD4T-N2, and CD4T-R harbor the EGFP, NBD1, NBD2, and R domain, respectively. (b) The indicated CD4T chimeras were transiently expressed in COS7 cells. Equal amounts of proteins were visualized by immunoblotting with anti-CD4 Ab. (c) Cell surface density of the indicated CD4T variants was measured by the immunoperoxidase assay, using primary anti-CD4 Ab and HRP-conjugated secondary Ab in live cells (see *Materials and Methods*). Amplex-Red fluorescence was normalized for cellular protein and expressed in arbitrary unit (a.u.). Means ± SEM, n ≥ 8. (d) Steady-state expression level of the CD4T chimeras was monitored by immunoblotting following proteasomes inhibition by MG132 (20 μM for 3 h) as indicated. (e) Cell surface expression of CD4T-λand CD4T-λ_m was measured by the immunoperoxidase assay (means ± SEM, n = 6). (f) Subcellular localization of CD4 chimera was detected by immunostaining with anti-CD4 Ab and Cy2-conjugated secondary Ab in transiently transfected COS7 cells. CD4-GFP was visualized by the EGFP fluorescence. The ER was visualized by anti-calnexin Ab (CNX) and rhodamine-conjugated secondary Ab in permeabilized cells (right). Plasma membrane was stained with WGA in nonpermeabilized cells. Single optical sections, obtained by fluorescence laser confocal microscopy are shown. Bar, 10 μm.

cell surface density of complemented R-M2-N2 and R*-M2-N2 fragments with M1-N1 and M1-N1*, respectively, reached 40–60% of the wt CFTR (Figure 1c). The cell surface density of CFTR severed at residue 388 was negligible in line with the immunoblotting data. All of the individually expressed C-terminal domain combinations failed to accumulate at the cell surface and were confined to the ER by calnexin (CNX) colocalization, suggesting that all these CFTR fragments are recognized as nonnative conformers by the ERAD (Figure 1, c and d).

Coexpression of M1-N1 + R-M2-N2 or M1 + N1-R-M2-N2 fragments conferred cAMP-stimulated plasma membrane halide conductance, a hallmark of CFTR channel activity, determined by the iodide efflux assay (Supplemental Figure S1b; data not shown). The N- and C-terminal fragments of CFTR were associated both at the early stage of their biosynthetic processing and in post-Golgi compartments (Supplemental Figure S1c; data not shown). Jointly, these observations indicate that severing CFTR at selected boundaries permits the channel assembly in mammalian cells and could be used to unravel the folding propensity of individual domains.

Cell-based Assay to Monitor the Conformation of CFTR Cytosolic Domains

We implemented an in vivo approach to assess the conformational maturation of CFTR cytosolic domains. The assay relies on the ability of the ER to recognize and degrade misfolded membrane proteins regardless whether the conformational defect is localized to the luminal, transmembrane or cytoplasmic domain and to target folded molecules to the cell surface (Vashist and Ng, 2004). The cytosolic domains of CFTR were tethered to transmembrane reporter molecules to ensure their surveillance by the ER quality control. We selected the truncated monomeric CD4 (CD4T) and invariant chain (IiT) as extensively used type I and type II model transmembrane proteins that lack specific sorting signals and are constitutively targeted to the plasma membrane (Piguet *et al.*, 1999; Barriere *et al.*, 2006).

The cell-based folding assay was validated by fusing the compactly folded enhanced green fluorescent protein (CD4T-GFP) and the intrinsically unstructured R domain (CD4T-R) to the CD4T cytoplasmic tail (Figure 2a). Immunoblotting analysis and cell surface anti-CD4 Ab binding with the immunoperoxidase fluorescence assay showed that the CD4T-GFP and CD4T have comparable cellular and plasma membrane expression levels (Figure 2, b and c), implying that EGFP attachment did not interfere with the biosynthetic processing efficiency of the reporter. In sharp contrast, the unstructured R domain chimera (CD4T-R) had negligible cell surface expression and was retained in the ER according to immunolocalization studies (Figure 2, b, c, and f). The conformational sensitivity of the cell-based trafficking assay was further verified by using chimeras containing the wild-type (wt) bacteriophage λ repressor N-terminal domain (CD4T-λ) and its temperature-sensitive mutant variant (CD4T-λ_m) (Pakula *et al.*, 1986). The L57G/L69G mutations decreased the melting temperature of the recombinant λ (molecular mass ~12 kDa) from 52 to 28°C (Pakula *et al.*, 1986). Unfolding of the λ_m domain at 37°C was sufficient to cause ER retention and the dramatic reduction in the cell surface expression of the CD4T-λ_m chimera (Figure 2, d and e).

The CD4T-R similar to the CD4T-λ_m was colocalized with CNX and calreticulin, ER-resident chaperones (Figure 2f; data not shown). In contrast, folded CD4T-λ and CD4T-GFP, similar to CD4T, were confined to the plasma membrane, indicated by colocalization with Alexa 594-conjugated WGA in nonpermeabilized cells (Figure 2f). Blocking the ERAD by the proteasome inhibitor MG132 augmented the cellular expression of the CD4T-λ_m, but not the CD4T-λ, and induced the accumulation of ubiquitinated adducts (Figure 2d; data not shown). Thus, the in vitro folding propensity of the domains correlates with the processing and cell surface ex-

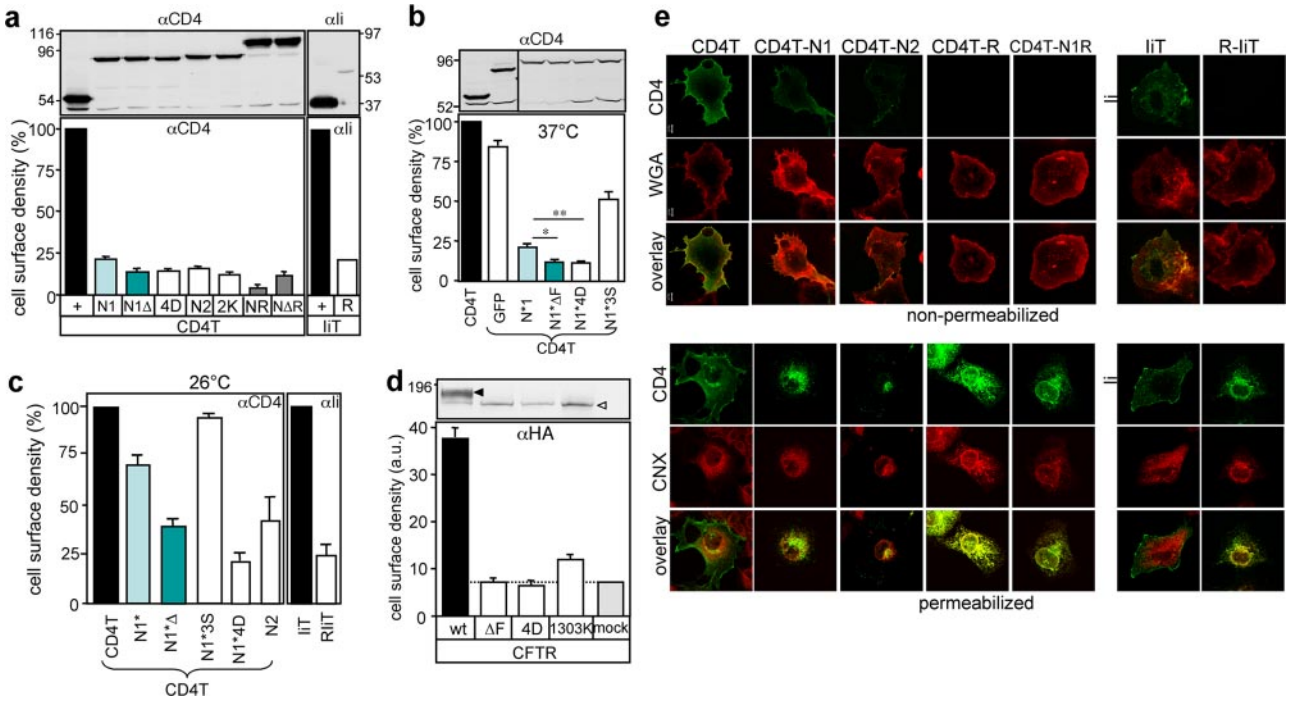

Figure 3. Biosynthetic processing of the chimeric CFTR cytosolic domains. (a) Immunoblot and cell surface detection of CD4 and Ii chimeras. The reporter molecules (CD4T and IiT) and the chimeras were transiently expressed in COS7 cells. Immunoblot and cell surface density analysis were performed with anti-CD4 (top left) and anti-Ii (top right) Abs. Cell surface density was expressed as percentage of CD4T or IiT after normalization of the fluorescence signal for cellular proteins. Abbreviations: N1ΔF, NBD1ΔF508; N14D, NBD1(L570D/L571D/I601D/L602D); N2K, NBD2(N1303K); N1R, NBD1-R; N1ΔR, ΔF508-NBD1-R (also see Supplemental Table S1). Means ± SEM, n ≥ 6. (b) Immunoblot and cell surface expression analysis of CD4 chimeras containing NBD1 with boundaries of the crystallized domain (N1*). The N1*ΔF and N1*4D contains the same mutations as defined in a. N1*3S incorporates the F429S, F494N, and Q637R solubilization mutations. Cell surface density and immunoblot analysis were performed as defined in a. Means ± SEM, n ≥ 5. Unpaired, two-tailed *t* test was used for comparisons. (*p = 0.0006, **p = 0.003; n = 11–15). (c) Cell surface expression of the CD4T and IiT chimeras was rescued at reduced temperature. The cell surface density of the indicated chimeras were measured as described in b, after culturing the cells for 24 h at 26°C. Means ± SEM, n = 3. (d) Expression and cell surface density of wt and mutant CFTR variants in stably transfected BHK cells, determined by immunoblotting and Ab binding assay, respectively. The core- and complex-glycosylated CFTR are depicted by empty and filled arrowhead, respectively. Means ± SEM, n = 3. (e) Indirect immunolocalization of CD4 and Ii chimeras in COS7 cells. Immunostaining of the chimeras with Alexa 594-WGA were performed in nonpermeabilized cells (top). Intracellular staining of the chimeras and CNX was established in permeabilized cells (bottom) as described in Figure 2f. Bar, 10 μm.

pression of the respective chimera, enabling us to monitor the conformational state of CFTR cytosolic domains in the cellular environment.

Biosynthetic Processing of Individual CFTR Domains Is Compromised

We tested one-, two-, three-, and four-domain combinations of CFTR, and only one of the four-domain combinations (see below) could bypass efficiently the ER quality control. By fusing the NBD1 and NBD2 to the COOH terminus of CD4T (CD4T-N1 and CD4T-N2) and the R domain to the invariant chain N terminus (R-IiT), we emulated the in situ topology of the cytosolic domains (Figure 1a). CD4T-N1 and CD4T-N2 incorporated the respective intracellular domains (ICD), whereas NBD1, encompassing the crystallization boundaries, was attached to the CD4T via a flexible linker (CD4T-N1*; Supplemental Table S1) (Barriere *et al.*, 2006). The chimeras were expressed with the predicted molecular masses in COS7 and BHK cells (Figure 3, a and b, and Supplemental Figure S2a). The following observations indicate that the NBD1, NBD2, and R domain chimeras were largely recognized as nonnative polypeptides by the ERAD machinery.

First, the chimeras cellular and cell surface expression was more than fourfold lower than the CD4T and IiT, determined by immunoblotting and cell surface Ab binding, respectively (Figure 3, a and b, and Supplemental Figure S2, a and b). Exposure of Tyr- and di-Leu-based endocytic signals unlikely accounts for this phenomenon, because the plasma membrane turnover of the chimeras was not accelerated (data not shown).

Second, although low level of cell surface expression of the N1-, N2-, and N1*-containing CD4 chimeras was detectable, most the chimeras were, predominantly, confined to the ER based on CNX and calreticulin colocalization in COS-7 and BHK cells (Figure 3e and Supplemental Figure S2c). No detergent-insoluble aggregates formation could be detected by immunoblotting (data not shown).

Third, the cell surface expression of the CD4T-N1* and CD4T-N2 was increased at 26°C by two- to threefold, suggesting that temperature-sensitive folding defect rather than linear peptide motif recognition accounts for the misprocessing (Figure 3c). Inhibition of proteasome activity by MG132 was unable to augment the cell surface expression of the chimeras (data not shown).

Four, introducing the ΔF508 or the N1303K (Gregory *et al.*, 1991) mutation in the NBD1 and NBD2, respectively, resulted in a small but significant decrease in the cell surface expression of CD4T-N1ΔF, CD4T-N1*ΔF, and CD4T-N2K compared with their wt counterparts (Figure 3, a and b, and

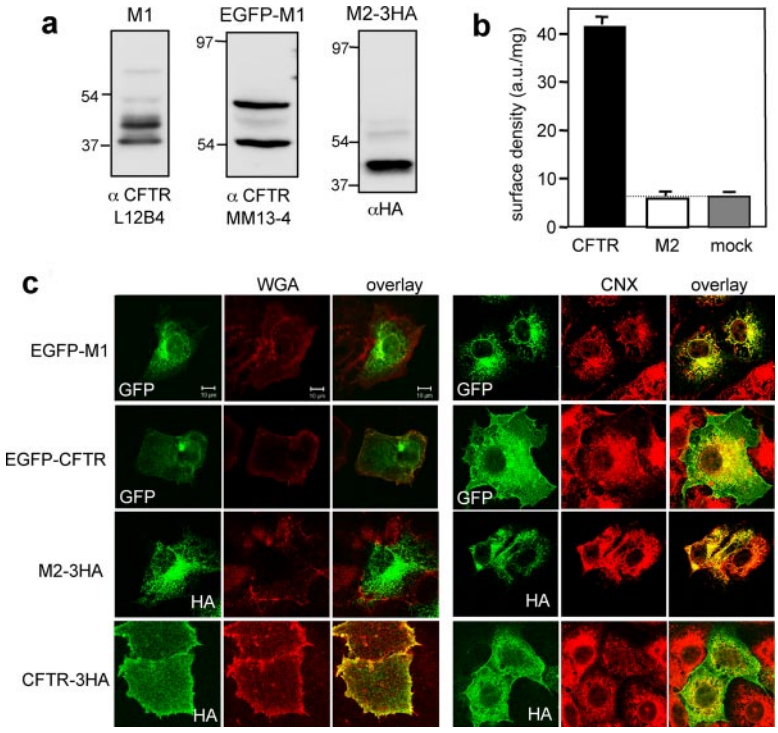

Figure 4. Intracellular retention of the MSD1 and the MSD2. The MSD1 (M1), EGFP-M1, and MSD2 (M2-3HA) were transiently expressed in COS7 cells. Immunoblotting (a) and cell surface density measurements (b) of MSD1, EGFP-MSD1, and MSD2-3HA (means ± SEM, n = 3). (c) Immunolocalization were performed as described in Figure 3e. Bar, 10 μm.

Supplemental Figure S2, b and c), implying that the mutations can amplify the ER-perceived folding defect. Similar results were obtained upon replacing four hydrophobic core residues with aspartic acids (4D: L570D/L571D/I601D/L602D) to disrupt the NBD1 folding (Figure 3, a and b, and Supplemental Figure S2b).

The 4D mutation, as the ΔF508 and N1303K, impaired the biosynthetic processing and global conformation of CFTR, according to immunoblotting, cell surface anti-HA Ab binding and limited proteolysis (Figure 3d and Supplemental Figure S3). The 4D mutation destabilized not only the NBD1, but also the MSD1 and NBD2 according to the chymotrypsin and trypsin resistance of the MSD1-, NBD1-, and NBD2-containing fragments (Supplemental Figure S3), resembling that effect of the ΔF508. The CD4T-N1*4D was less amenable to low-temperature rescue, conceivable due to its severe folding defect (Figure 3c).

Five, remarkably, introducing three solubilization mutations (F429S, F494N, and Q637R) that were required to produce soluble, recombinant NBD1 in bacteria (Lewis *et al*., 2005), significantly increased the steady-state cell surface expression of the CD4Tl-N1*-3S at 37°C and suppressed the expression defect at 26°C (Figure 3, b and c). The solubilization mutations increased the melting temperature of the isolated NBD1 by >5°C and decreased the ubiquitination susceptibility of the chimera (Rabeh, Du, and Lukacs, unpublished observations).

The R domain was largely recognized as a nonnative polypeptide regardless of the reporter molecule, as indicated by the 80% reduced the cell surface expression and ER retention of the CD4T-R and R-IiT in a temperature-independent manner (Figures 1c and 3a, c, and e).

The subcellular distribution of the membrane spanning domains MSD1 (M1 and M1*) and MSD2 (M2) was established by the EGFP- and 3HA-tagged variants (Benharouga *et al*., 2003; Sharma *et al*., 2004), respectively (Figure 4). The boundaries of MSDs were modified to increase the expression levels (Supplemental Table, Figure 4a, and Supplemental Figure S4c). M1, M1*, and M2 were retained in the ER and failed to accumulate at the cell surface contrary to the EGFP- or 3HA-tagged CFTR (Figure 4, b and c). These observations suggest that the individually expressed CFTR domains are, predominantly, recognized as nonnative polypeptides by the ER quality control.

Two and Three-Domain Combinations of CFTR Fail to Attain Native Conformation

CFTR domain assembly may be required to mask nonpolar or hydrophobic residues in the cytoplasm and/or to bury or expose linear trafficking motifs recognizable by the ER retention and export machinery, respectively. Domain–domain interactions may also optimize the folding energetics by cooperatively stabilizing domains as observed in a subset of multidomain soluble proteins (Wenk *et al*., 1998; Han *et al*., 2007). This may determine the channel ER export efficiency similar to that described for secretory proteins (Wiseman *et al*., 2007). To address some of these mutually nonexclusive possibilities, the biosynthetic processing and cell surface expression of two- and three-domain combinations were determined. We found that none of the two- or three-domain combinations could efficiently bypass the ER quality control, although very low level expression could be detected (Supplemental Figure S4; also see Figures 1C and 5A).

Replacement of critical Arg with Lys residues in the MSD1 (R29K) and NBD1 (R516K and R555K) failed to revert the processing defect of M1(RK) and M1-N1(3RK) (Supplemental Figure S5), whereas it partially rescued the ΔF508 CFTR ER retention (Owsianik *et al*., 2003; Roxo-Rosa *et al*., 2006). Therefore, exposure of RXR ER retention motifs cannot account for the processing defect of the MSD1-NBD1.

The De Novo Folding Unit of CFTR

The cellular fate of four-domain assemblies was assessed next. CFTR variants lacking a single domain (ΔMSD1: N1-

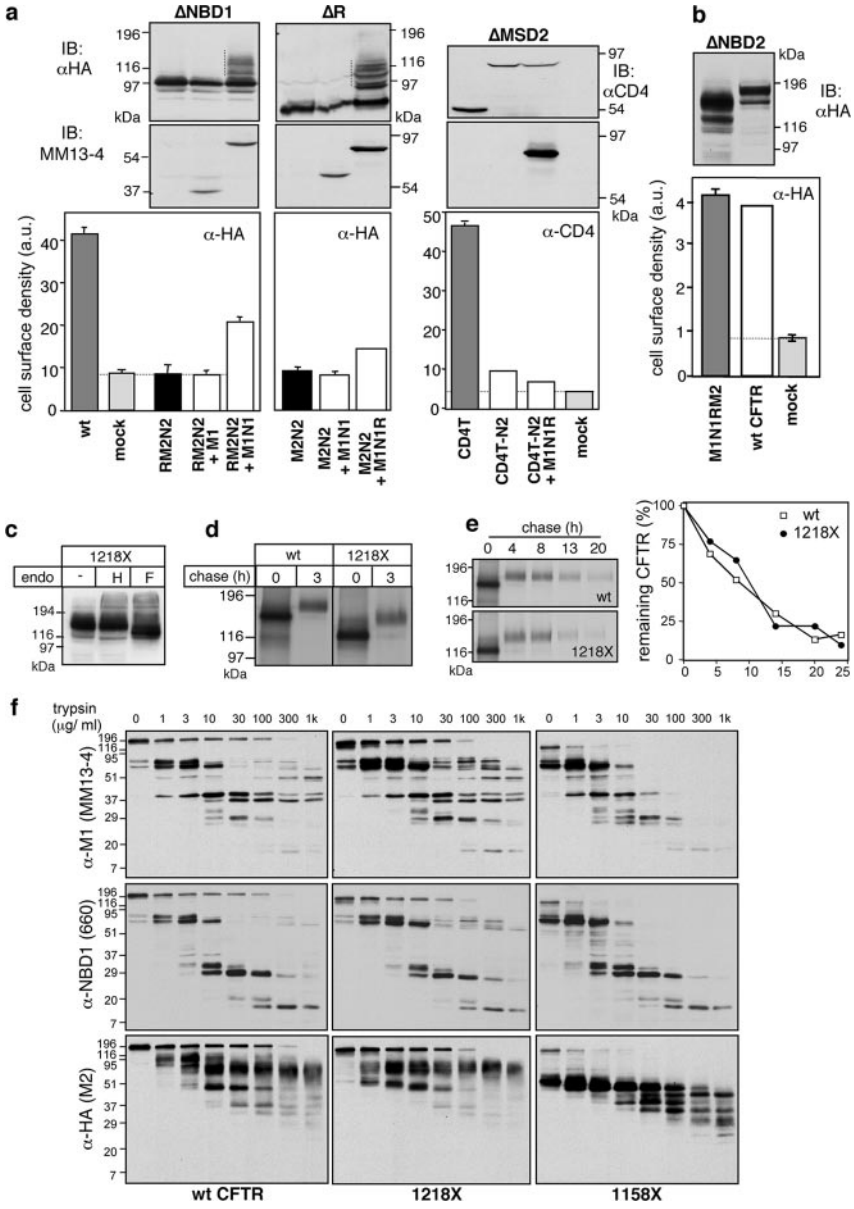

Figure 5. Expression and characterization of CFTR four-domain combinations. CFTR constructs lacking the indicated domain (ΔNBD1, ΔR, and ΔMSD2) (a) and ΔNBD2 (b) were expressed as M1 + RM2N2, M1N1 + M2N2, M1N1R + CD4T-N2, and M1N1RM2 (CFTR-1218X), respectively, in COS7 cells. Equal amounts of cell lysates were immunoblotted (top). Split wt CFTR was expressed as control, demonstrating the electrophoretic mobility shift of the complex-glycosylated R2M2N2 and M2N2 (dotted line) in the presence of complementing N-terminal fragments. The cell surface density of the M2 containing CFTR fragments, wt CFTR, and CD4T-N2 was measured by the immunoperoxidase assay (bottom). Means ± SEM, n = 3. (c) CFTR-1218X is complex-glycosylated. Cell lysates were treated with the endoglycosidase H or Endo F. Immunoblotting was performed with anti-HA Ab. (d) Maturation efficiency of CFTR-1218X was measured by metabolic pulse-chase experiments in stably transfected BHK cells. After a 10-min pulse labeling, cells were chased for 3 h, and CFTR was immunoprecipitated and visualized by fluorography. (e) Metabolic stability of the complex-glycosylated CFTR-1218X. Pulse-labeled BHK cells were chased as indicated, and labeled CFTR was visualized by fluorography and quantified by phosphorimage analysis by using the ImageQuant software (right). (f) In situ protease susceptibility of the wt and C-terminally truncated CFTR. Microsomes from wt, 1218X-, and 1158X CFTR-expressing BHK cells were subjected to limited proteolysis at the indicated trypsin concentration for 15 min on ice. Digestion patterns of CFTR were visualized by immunoblotting with MSD1-, NBD1-, and MSD2-specific anti-CFTR monoclonal Abs.

R-M2-N2; ΔNBD1: M1 + R-M2-N2; ΔR: M1-N1 + M2-N2; ΔMSD2: M1-N1-R + CD4T-N2; or ΔNBD2: CFTR-1218X) were expressed as split molecule or linear polypeptide. Based on electrophoretic mobility shift and cell surface Ab binding, deletion of the NBD2 was the only four-domain assembly that accumulated efficiently at the cell surface (Figure 5, a and b; also see Figure 1a, lanes 6; b, lanes 7–9; and c and d).

The CFTR-1218X has several hallmarks of the wt CFTR. 1) CFTR-1218X was complex-glycosylated and Endo-H resistant, confirming recent observations (Cui *et al*., 2007) (Figure 5c). 2) Although CFTR-1218X has slightly decreased folding efficiency relative to its wt counterpart, the metabolic stability of the wt and mature CFTR-1218X ($t_{1/2} \approx 10$ h) was comparable (Figure 5, d and e). 3) Deletion of the NBD2 failed to alter the global protease susceptibility of the CFTR-1218X as well as the MSD1-, NBD1-, and MSD2-containing fragments (Figure 5f). The protease resistance of CFTR variants was measured in isolated microsomes by visualizing the proteolytic cleavage pattern with domain-specific antibodies (Figure 5f and Supplemental Figure S6a; data not shown). 4) The protein kinase A (PKA)-stimulated halide conductance of CFTR-1218X–expressing cells confirmed that the channel was partially functional at the plasma membrane (Cui *et al*., 2007) (Supplemental Figure S6b).

The notion that the four-domain assembly may represent the minimal folding unit of CFTR is supported by the following observations. 1) Disrupting the integrity of the MSD2 by truncating at the TM11–12 segment (CFTR-1097X, -1041X, and -1128X) or at the C-terminal cytosolic interface (CFTR-1158X but not CFTR-1174X) abrogated the processing and caused ER retention of the channel (Supplemental Figure S6, c and d). 2) Remarkably, truncation of the MSD2 C terminus (CFTR-1158X) not only increased the global protease susceptibility of the channel and the MSD2 but also the MSD1 (Supplemental Figure 5f), implying that the MSD1 conformational stability is dependent on the MSD2 structure. 3) The processing of CFTR-1218X could be reconstituted from two complementary segments, consisting of M1-N1 + R-M2 or M1 + N1-R-M2, measured by three different assays (Fig-

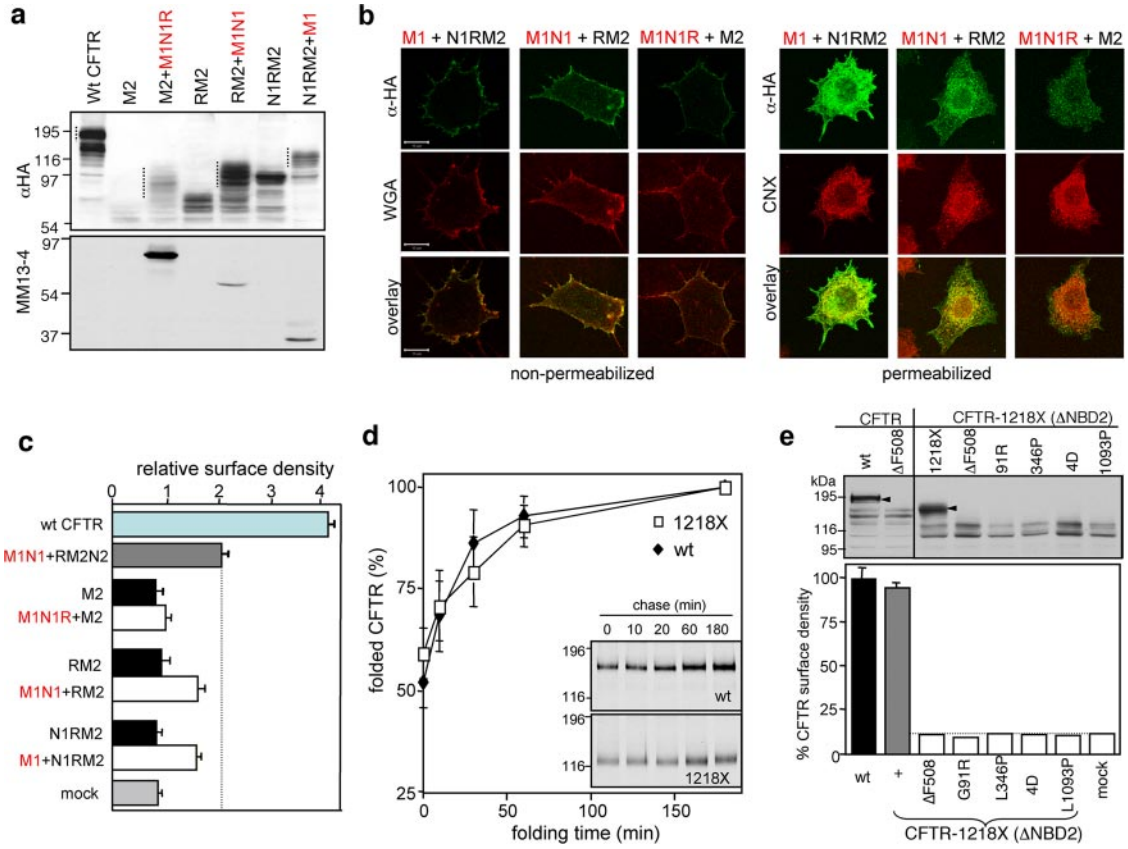

Figure 6. Biosynthetic processing and the folding kinetics of the CFTR-1218X variants. (a) Processing of the split CFTR-1218X. Complex-glycosylation of M2 containing fragments of CFTR-1218X was restored in the presence of complementary N-terminal fragments in transiently transfected COS7 cells. The C- and N-terminal CFTR fragments were visualized by immunoblotting using the anti-HA and MM13-4 Ab, respectively. Dotted line indicates the complex-glycosylated form. (b) Immunolocalization of the M2 containing fragments in cells expressing the indicated N- and C-terminal fragments of the CFTR1218X. Colocalization with Alexa594-WGA and CNX, plasma membrane and ER markers, respectively was performed as described in Figure 1d. Bar, 10 μm. (c) Cell surface density of the M2 containing fragments of COS7 cells transiently expressing the C- and N-terminal fragments of split CFTR-1218X. The immunoperoxidase assay was performed with anti-HA Ab. Wt CFTR and its split variant (M1N1 + RM2N2) were used as positive controls. Means ± SEM, n = 3. (d) Folding kinetics of wt and 1218X CFTR. Stably transfected BHK cells were pulse labeled for 8 min with [^{35}S]methionine and [^{35}S]cysteine and chased in BFA (10 μg/ml) containing medium for 3 h (inset). Folding was terminated by depleting the cellular ATP content as described in *Materials and Methods*. CFTR was immunoprecipitated and visualized by fluorography (inset). The CFTR radioactivity was quantified by phosphorimage analysis. Similar results were obtained in the absence of BFA. Data are means (±SEM, n = 5) and expressed as percentage of the maximum amount of radioactivity associated with CFTR. (e) Missense mutations provoke the intracellular retention of the CFTR-1218X. COS7 cells were transiently transfected with the indicated construct and biosynthetic processing was visualized by the accumulation of the complex-glycosylated form (arrowhead) with immunoblotting (top). All the mutants remained core-glycosylated. Cell surface density of CFTR-1218X variants was measured by anti-HA Ab binding assay as described in Figure 2c (bottom).

ure 6, a–c). Although these fragments alone were unable to escape the ER, coexpression assured comparable surface expression to that of the split wt CFTR (Figure 6c), indicating that individually translated domains can assemble into the native fold. The interaction between the two fragments of the CFTR-1218X was preserved in post-ER compartments and cannot be attributed to postlysis artifact according to coimmunoprecipitations (Supplemental Figure S6e).

Successfully restoring the biosynthetic processing of the split CFTR-1218X is consistent with the notion that individually translated domain combinations complete their folding posttranslationally. To confirm this inference, the wt and CFTR-1218X conformational maturation kinetics were compared in vivo. After an 8-min pulse labeling and a 5- to 60-min chase, folding was terminated by cellular ATP depletion (Lukacs *et al*., 1994; Du *et al*., 2005). ATP-depletion ensured complete elimination of nonnative CFTR without altering the stability (Lukacs *et al*., 1994) and aggregation propensity of the folded wt and CFTR-1218X, as indicated by quantitative recovery of folded core- and complex-glycosylated CFTR with nondenaturing immunoprecipitation (Supplemental Figure S6f). The accumulation of wt and CFTR-1218X was completed in ~40 min after the pulse labeling (Figure 6d), indicating that the de novo folding of the four-domain assembly (CFTR-1218X), similar to wt CFTR, is completed posttranslationally.

Point Mutations Cause Cooperative Misfolding of CFTR Domains

Although the domain-wise folding mechanism implies that structural perturbation of individual CFTR domain is restricted to the mutant domain (Kleizen *et al*., 2005), involvement of cooperative domain folding predicts that point mutations would interfere with the folding and/or stability of multiple domains (i.e., cooperative misfolding). This prediction was tested by examining the domain-wise conforma-

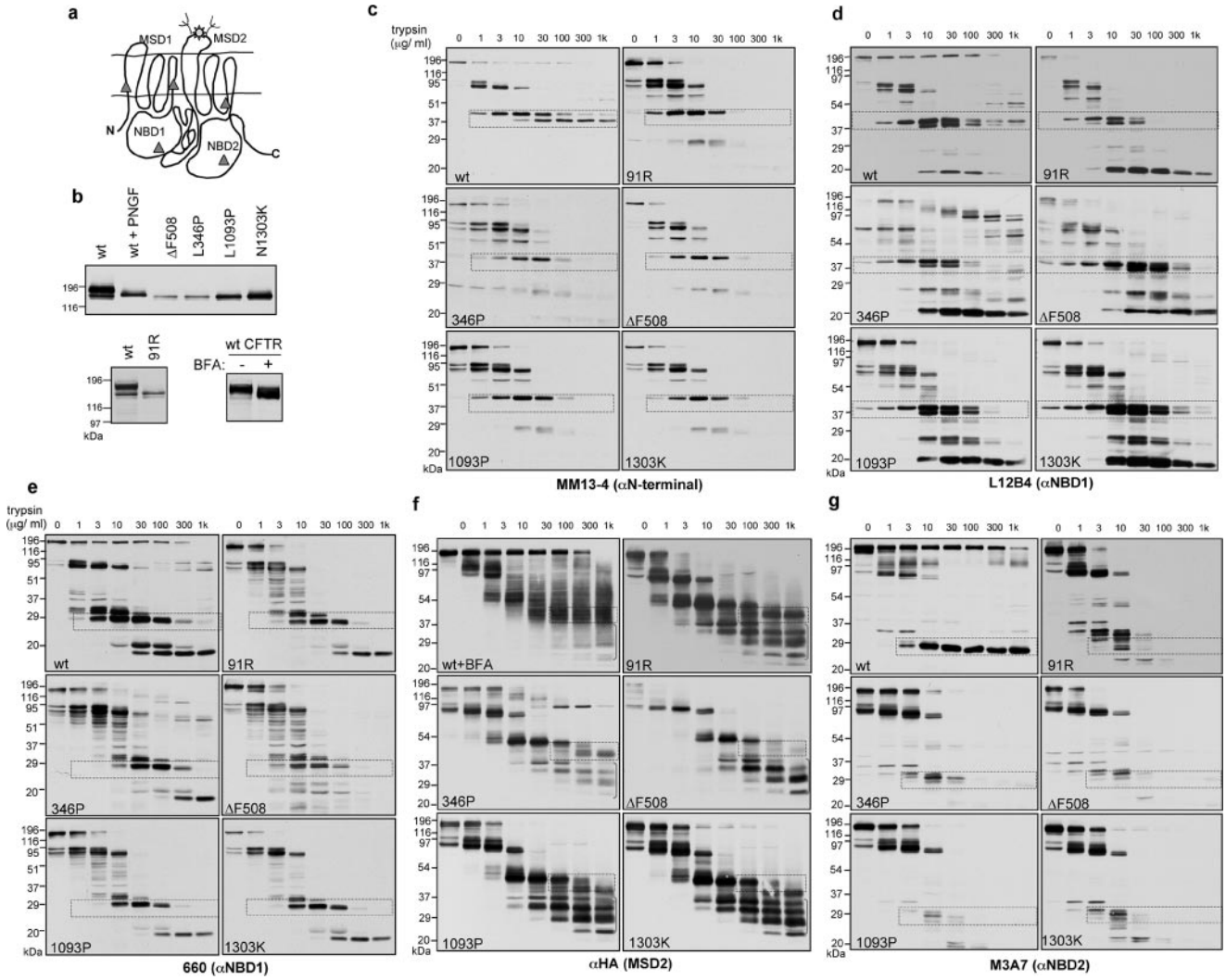

Figure 7. Global and domain-wise conformational perturbations of CFTR variants harboring missense mutations. (a) Schematic localization of CF associated point mutations in CFTR used in this study. (b) Point mutations prevent the biosynthetic processing of CFTR detected by immunoblotting in stably transfected BHK cells. Equal amounts of cell lysates were probed with anti-HA Ab. The BFA-induced accumulation of the folded, core-glycosylated wt CFTR in cells exposed to BFA for 24 h is illustrated by immunoblotting (bottom right). (c–g) Comparison of the in situ trypsin susceptibility of wild type and mutant CFTRs. Isolated microsomes expressing the indicated CFTR variant were digested at the indicated concentration of trypsin as described in Figure 6f. CFTR proteolytic fragments were visualized by immunoblotting with the following antibodies: anti-N-MSD1 (MM13-4; c), anti-NBD1 (L12B4; d), anti-NBD1 (660; e); anti-HA (MSD2 specific; f), and anti-NBD2 (M3A7; g). The proteolytic degradation intermediate representing the MSD1-, NBD1-, MSD2- and NBD2-containing fragment, based on multiple epitope localization, molecular masses and ATP binding are indicated by rectangles (Du *et al*., 2005; Cui *et al*., 2007). Note that in f, proteolytic digestion was performed on microsomes isolated from BFA-treated wt CFTR-expressing BHK cell to facilitate comparison of the core-glycosylated wt MSD2 with its mutant counterparts.

tional defect of CFTR by mutations in the MSD1, MSD2, NBD2, and NBD1 (ΔF508 and 4D). Four CF mutations, G91R (Xiong *et al*., 1997), L346P (Choi *et al*., 2005), L1093P (Seibert *et al*., 1996), and N1303K (Gregory *et al*., 1991), localized to the transmembrane (TM) 1 and TM6 in MSD1, the cytosolic loop (CL) 4, and in the NBD2, respectively (Figure 7a). Expression analysis by immunoblotting in stably transfected BHK cells confirmed that the mutants remained core-glycosylated and failed to accumulate at the cell surface similar to the ΔF508 and 4D-CFTR (Figure 7b; data not shown).

CFTR global and local structural stability was probed by limited proteolysis, by using NBD1 (L12B4 and 660), NBD2 (M3A7), MSD1 (MM13-4), and MSD2 (anti-HA)-specific monoclonal antibodies (Kartner and Riordan, 1998; Cui *et al*., 2007). The conformational stability of the NBD1-, NBD2-, and MSD1-containing polypeptide fragments was measured based on their protease resistance. The identity of the respective fragments was validated previously (Du *et al*., 2005; Cui *et al*., 2007). To rule out that the accessibility of single cleavage site provoked cooperative unfolding, both chymotrypsin and trypsin digestion was performed and yielded similar results (Figure 7, c–f, and Supplemental Figure S7.)

All of the mutations led to global destabilization of CFTR, indicated by a 10- to 50-fold increased protease sensitivity of the full-length CFTR (Figure 7, c–g). The MM13-4, N-terminal specific Ab probed the 37- to 42-kDa N-MSD1–containing fragments protease susceptibility. All the five mutations prevented the 37-kDa immunoreactive polypeptide accumulation, conceivably by exposing additional cleavages sites in the MSD1, indicated by the transient accumulation of a 27-

to 29-kDa degradation intermediate (Figure 7c and Supplemental Figure S7).

Mutations caused a modest increase in the protease susceptibility of the NBD1-containing fragment or its degradation intermediates (~29 and ~39 kDa, detected by the 660 and L12B4 Ab, respectively; Figure 7, d and e, and Supplemental Figure S7).

The protease susceptibility of the mutant, core-glycosylated MSD2 was compared with that of the native, core-glycosylated wt CFTR, accumulated in the ER in BFA-treated cells (Lukacs *et al*., 1994) (Figure 7b). The ~45-kDa anti-HA Ab-reactive polypeptide represents the MSD2-containing fragment, considering that R-domain–specific epitopes were eliminated at low protease concentration (Figure 7f; data not shown). All of the mutations profoundly increased the MSD2 protease susceptibility and induced the accumulation of ~22- to 37-kDa immunoreactive degradation intermediates (Figure 7f).

Remarkably, the G91R, L346P, ΔF508, 4D, and L1093P mutations, regardless of their location, profoundly augmented the protease susceptibility of the NBD2 (~30 kDa), probed with the M3A7 Ab (Figure 7g and Supplemental Figure S7c). These observations, jointly, imply that conformational defect caused by mutations is not restricted to the mutant domain, but spread to multiple CFTR domains. Considering that the biosynthetic processing of the CFTR-1218X was invariably prevented by the mutation residing in the MSD1, NBD1, and MSD2 (Figure 6e), it is tempting to speculate that the four-domain folding unit serves as an intramolecular scaffold to facilitate the NBD2 posttranslational folding that ultimately contributes to the stability of the full-length CFTR. Small structural perturbations in individual domains are amplified by cooperative misassembly of the four-domain folding unit, preventing the conformational maturation NBD2 that in turn contributes to global misfolding.

DISCUSSION

Although domain-wise, cotranslational folding is envisioned as the predominant folding mechanism of soluble multidomain proteins, as well as CFTR in mammalian cells (Frydman *et al*., 1999; Nicola *et al*., 1999; Kleizen *et al*., 2005), accumulating observations suggest that a subset of polypeptides undergoes cooperative domain folding (Han *et al*., 2007). Although domain interactions have been recognized to contribute to CFTR biogenesis (Du *et al*., 2005; Thibodeau *et al*., 2005; Younger *et al*., 2006; Cui *et al*., 2007; Rosser *et al*., 2008), here we demonstrate that the minimal folding unit of CFTR is composed of N1M1RM2. Furthermore, evidence is provided in support of the cooperative domain folding involvement in CFTR biogenesis.

Systematic analysis of the domain requirement that is necessary and sufficient to attain native-like CFTR architecture revealed that coexpression of MSD1, NBD1, R, and MSD2 was essential either as a linear or a split polypeptide to ensure that the domains are recognized as native entities by the ER quality control. The single-, two-, or three-domain combinations were unable to escape efficiently the ER quality control in both BHK and COS7 cells, suggesting that they are energetically and conformationally destabilized. Similar observations were made in human bronchial epithelia, indicating that the interdependent domain folding is not cell specific (data not shown). Notably, the slow folding kinetics of the four-domain folding unit coincided with the posttranslational assembly of the NBD2 and wt CFTR folding (Du *et al*., 2005) (Figure 7d).

Multiple mechanisms were considered to account for the surprising observation that all the domains and most of their combinations inefficiently or not at all escape the ER quality control. Involvement of the RXR motifs was ruled out to account for the ER retention because the processing defect of the MSD1-NBD1 could not be reversed by mutating the RXR ER-retention motif (Supplemental Figure S5). Another possibility is that exposed interdomain interface, enriched in nonpolar and hydrophobic residues are recognized by the ER quality control machinery (Gilon *et al*., 1998; Ellgaard and Helenius, 2003; Anelli and Sitia, 2008). Depending on the amino acid packing density and hydrophobicity at the interface, this mechanism itself or in combination with energetic destabilization may lead to inefficient export from the ER (Wiseman *et al*., 2007). Although thermodynamic and kinetic analysis of domain assemblies of CFTR has not been performed, biophysical measurements showed interdependent domain folding kinetics and stability in soluble multidomain proteins and their perturbation by point mutations at interdomain interfaces (Wenk *et al*., 1998; Klein-Seetharaman *et al*., 2002; Han *et al*., 2007). A similar cooperative folding paradigm may prevail in a subset of membrane proteins, including the CFTR, suggesting that individual domains are thermodynamically stabilized upon their assembly. In support of this hypothesis, severalfold increase in the cell surface expression of CD4T-NBD1* was documented in the presence of those solubilization mutations (F429N, F494N, and Q637R) that were required for the recombinant NBD1 expression (Figure 3, b and c) (Lewis *et al*., 2005). The F494 residue is likely to be engaged in van der Waals interactions with residues at the MSD2 and NBD2 interface (He *et al*., 2008; Mornon *et al*., 2008; Serohijos *et al*., 2008a). Indeed, the F429N, F494N, and Q637R mutations thermodynamically stabilized the isolated NBD1 in the absence of domain-domain interactions as indicated by the elevated melting temperature of the recombinant NBD1*-3S relative to its wt counterpart (Rabeh, Mulvihille and Lukacs, unpublished observations). Domain stabilization may also prevail in vivo, supported by the high level of cell surface expression and decreased ubiquitination of the CD4T-N1*-3S at 37 and 26°C compared with that of the CD4T-N1* (Figure 3, b and c; data not shown).

The observation that the NBD2 is not required for the CFTR-1218X conformational maturation is surprising but is consistent with previous results (Cui *et al*., 2007; Wang *et al*., 2007a,b). Although deletion of the NBD2 is predicted to expose the N2/N1 and N2-M1/M2 interface (≈7245 Å^2) (Mornon *et al*., 2008; Serohijos *et al*., 2008a), this scenario is unlikely, considering the preserved protease resistance of the NBD1, MSD1, and MSD2 in CFTR-1218X. Notably, truncations of the MSD2 C terminus not only increased the protease susceptibility of the MSD2 but also the NBD1 and MSD1 (Figure 5f), consistent with the increased ubiquitination propensity of the MSD1-NBD1-R after the MSD2 truncation (Younger *et al*., 2006). It is possible that rearrangement of the intrinsically unstructured R domain protects the exposed interdomain interface in the CFTR-1218X, although this hypothesis awaits verification.

Deletion of the R domain C-terminal region (residues 708-835) was dispensable, but elimination of the R domain beyond 708 residues (ΔR-CFTR) prevented or dramatically reduced CFTR processing in mammalian cells (Winter and Welsh, 1997; Chappe *et al*., 2005), in line with our results. The dispensable nature of the R domain C-terminal region in CFTR biogenesis is conceivably due to its intrinsically disordered structure and low-affinity intramolecular interactions, indicated by in vitro, in vivo, and in silico studies

(Winter and Welsh, 1997; Ostedgaard *et al*., 2000b; Baker *et al*., 2007; Hegedus *et al*., 2008).

One of the most important observations of this study is that the NBD2 conformational stability was dramatically impaired regardless the localization of mutations (G91R, L346P, ΔF508, 4D, and L1093P) in the NBD1, TM1, TM6, or CL4 (Figure 6e). Because all these mutations disrupted the four-domain folding unit (CFTR-1218X) biogenesis (Figure 7e) and by inference multiple domain conformation, the simplest interpretation is that the four-domain folding unit serves as an intramolecular scaffold assisting the NBD2 folding/stabilization upon the formation of interdomain interface with CL1, CL2, and CL3 (Du *et al*., 2005; He *et al*., 2008). Nevertheless, considering that the N1303K mutation increased the protease susceptibility of both the MSD1 and MSD2 and deletion of the NBD2 modestly diminished the maturation efficiency of the CFTR-1218X as well as prevented the low-temperature rescue of the ΔF508-CFTR-1218X–processing defect (Supplemental Figure S8), we propose that NBD2 contributes to the global stabilization CFTR despite that it is nonessential for the channel processing.

Several observations favor the explanation that CFTR assemble requires cooperative domain folding. 1) CFTR individual domains and two-, three- and four-domain combinations (except the M1-N1-R-M2) were recognized largely as nonnative entities, leading to severely reduced processing efficiency, ER retention, and degradation. Simultaneous expression of the M1-N1-R-M2 domain combination as a linear or split polypeptide was necessary and sufficient to confer stability and native-like state to the domains and render them in vivo stability (Figures 3–5). Likewise, although individual halves of split CFTR were trapped in the ER, efficient complementation of the full-length CFTR processing was observed (Figure 1c). Complementation of the processing defect of the ΔF508-CFTR with the M1-N1 fragment, but not with the ΔF508-M1-N1 fragment, is consistent with the critical role of specific domain–domain interactions in folding (Cormet-Boyaka *et al*., 2004). 2) The N1303K NBD2 mutation disrupted the full-length CFTR export, as well as the MSD1 and MSD2 conformation, measured by the in situ protease susceptibility assay, emphasizing that the NBD2 stabilizes some of the N-terminal domains. 3) Single point mutations in the NBD1, MSD1, and MSD2 caused conformational defect in two or three other domains, as well as destabilization, ER retention, and degradation of the channel. The ΔF508 mutation has marginal structural effect on the NBD1 domain, whereas it severely destabilized the MSD1, MSD2, and NBD2 (Figure 7). The simplest interpretation of these results is that a point mutation due to the domain-interdependent or cooperative folding pathway disrupts the stability of multiple domains. This mechanism also offers an explanation for the misprocessing of large number of missense mutations dispersed along the full-length CFTR (Zielenski and Tsui, 1995).

Cooperative misfolding is predicted to amplify relatively modest and localized structural defects caused by point mutations (e.g., L346P and ΔF508). The L346P mutation destabilizes the TM5/6 hairpin in vitro by decreasing intrahelical H^+ bondings and the TM6 helix net hydrophobicity that could be reverted by a suppressor mutation (Choi *et al*., 2005). The hairpin instability manifested in the MSD1 and MSD2 conformational defect and subsequently impaired NBD2 folding, demonstrated here by the protease hypersensitivity of these domains.

The global conformational defect of the ΔF508 CFTR, initiated by localized perturbation of NBD1 structural dynamics (Lewis *et al*., 2005), also underlines the cooperative nature of the channel misfolding mechanism. The ΔF508 mutation manifests in decreased folding yield in vitro (Thibodeau *et al*., 2005), modestly increased protease susceptibility in vivo (Du *et al*., 2005; Cui *et al*., 2007), and minimal structural perturbations in vitro (Lewis *et al*., 2005). Molecular dynamics modeling predicted the impaired folding kinetics and the destabilization of the S6-H7 loop of the ΔF508-NBD1 (Serohijos *et al*., 2008b). The long-range consequence of the modest structural defect in ΔF508 NBD1, exacerbated by the absence of the F508 side chain interactions (Serohijos *et al*., 2008a), could be explained by the cooperative domain misfolding. This leads to the misfolding of the MSD1 and NBD2 (Du *et al*., 2005; Cui *et al*., 2007; He *et al*., 2008), as well as the MSD2 destabilization, demonstrated here for the first time (Figure 7f). The global conformational defect of the ΔF508-CFTR and other mutants serves as efficient recognition and degradation signal for the ERAD (Figure 7, c–g) (Meacham *et al*., 2001; Younger *et al*., 2006; Nakatsukasa and Brodsky, 2008).

In summary, we outlined a folding model involving cooperative domain assembly as a necessary step to confer native tertiary structure to the CFTR. The cotranslational domain folding is facilitated by cytosolic and ER chaperones and generates loosely folded conformers (Kleizen *et al*., 2005), maintained in their folding competent state via chaperone interactions (Nakatsukasa and Brodsky, 2008). Compactly folded domain assemblies of both the wt and 1218X-CFTR are, however, attained posttranslationally. This process presumably coincides with the formation of native interdomain interfaces and thermodynamic stabilization of individual domains. The cooperative domain assembly offers a plausible explanation for the cooperative misfolding of multiple domains caused by several CF mutations, a mechanism that conceivably contributes to other ABC transporter biogenesis as well. This inference is supported by the isolation of suppressor mutations in the MSD1, MSD2, and NBD2 of the yeast cadmium factor ABC transporter with phenotypic mutation in its NBD1 (Falcon-Perez *et al*., 2001). Similar observations were reported in the Yor1p ABC transporter (Pagant *et al*., 2008).

ACKNOWLEDGMENTS

We thank J. Young and members of the Lukacs laboratory for careful reading of the manuscript and helpful suggestions, M. Bagdany for generating the RXR mutations, J. Riordan and A. Badwell for providing anti-CFTR antibodies, and A. Davidson and C. A. Kaiser for the λ cDNA. Work was supported by grants from the Cystic Fibrosis Foundation Therapeutics, the CCFF, the Canadian Institutes of Health Research, the National Institutes of Health (National Institute of Diabetes and Digestive and Kidney Diseases), and the Canadian Foundation for Innovation. G.L.L. is a holder of a Canada Research Chair.

REFERENCES

Anelli, T., and Sitia, R. (2008). Protein quality control in the early secretory pathway. EMBO J. *27*, 315–327.

Ashman, J. B., and Miller, J. (1999). A role for the transmembrane domain in the trimerization of the MHC class II-associated invariant chain. J. Immunol. *163*, 2704–2712.

Baker, J. M., Hudson, R. P., Kanelis, V., Choy, W. Y., Thibodeau, P. H., Thomas, P. J., and Forman-Kay, J. D. (2007). CFTR regulatory region interacts with NBD1 predominantly via multiple transient helices. Nat. Struct. Mol. Biol. *14*, 738–745.

Barriere, H., Nemes, C., Du, K., and Lukacs, G. L. (2007). Plasticity of polyubiquitin recognition as lysosomal targeting signals by the endosomal sorting machinery. Mol. Biol. Cell *18*, 3952–3965.

Barriere, H., Nemes, C., Lechardeur, D., Khan-Mohammad, M., Fruh, K., and Lukacs, G. L. (2006). Molecular basis of oligoubiquitin-dependent internalization of membrane proteins in mammalian cells. Traffic *7*, 282–297.

Benharouga, M., Sharma, M., So, J., Haardt, M., Drzymala, L., Popov, M., Schwapach, B., Grinstein, S., Du, K., and Lukacs, G. L. (2003). The role of the C terminus and Na+/H+ exchanger regulatory factor in the functional expression of cystic fibrosis transmembrane conductance regulator in nonpolarized cells and epithelia. J. Biol. Chem. *278*, 22079–22089.

Chan, K., Csanady, L., Seto-Young, D., Nairn, A., and Gadsby, D. (2000). Severed molecules functionally define the boundaries of the cystic fibrosis transmembrane conductance regulator's NH(2)-terminal nucleotide binding domain. J. Gen. Physiol. *116*, 163–180.

Chang, X. B., Cui, L., Hou, Y. X., Jensen, T. J., Aleksandrov, A. A., Mengos, A., and Riordan, J. R. (1999). Removal of multiple arginine-framed trafficking signals overcomes misprocessing of delta F508 CFTR present in most patients with cystic fibrosis. Mol. Cell *4*, 137–142.

Chappe, V., Irvine, T., Liao, J., Evagelidis, A., and Hanrahan, J. W. (2005). Phosphorylation of CFTR by PKA promotes binding of the regulatory domain. EMBO J. *24*, 2730–2740.

Choi, M. Y., Partridge, A. W., Daniels, C., Du, K., Lukacs, G. L., and Deber, C. M. (2005). Destabilization of the transmembrane domain induces misfolding in a phenotypic mutant of cystic fibrosis transmembrane conductance regulator. J. Biol. Chem. *280*, 4968–4974.

Cormet-Boyaka, E., Jablonsky, M., Naren, A. P., Jackson, P. L., Muccio, D. D., and Kirk, K. L. (2004). Rescuing cystic fibrosis transmembrane conductance regulator (CFTR)-processing mutants by transcomplementation. Proc. Natl. Acad. Sci. USA *101*, 8221–8226.

Cui, L., Aleksandrov, L., Chang, X. B., Hou, Y. X., He, L., Hegedus, T., Gentzsch, M., Aleksandrov, A., Balch, W. E., and Riordan, J. R. (2007). Domain interdependence in the biosynthetic assembly of CFTR. J. Mol. Biol. *365*, 981–994.

Du, K., and Lukacs, G. (2007). Cooperative domain assembly is essential for CFTR folding in living cells. Pediatr. Pulmonol. *42*, 204.

Du, K., Sharma, M., and Lukacs, G. L. (2005). The DeltaF508 cystic fibrosis mutation impairs domain-domain interactions and arrests post-translational folding of CFTR. Nat. Struct. Mol. Biol. *12*, 17–25.

Ellgaard, L., and Helenius, A. (2003). Quality control in the endoplasmic reticulum. Nat. Rev. Mol. Cell Biol. *4*, 181–191.

Falcon-Perez, J. M., Martinez-Burgos, M., Molano, J., Mazon, M. J., and Eraso, P. (2001). Domain interactions in the yeast ATP binding cassette transporter Ycf1p: intragenic suppressor analysis of mutations in the nucleotide binding domains. J. Bacteriol. *183*, 4761–4770.

Frydman, J., Erdjument-Bromage, H., Tempst, P., and Hartl, F. (1999). Co-translational domain folding as the structural basis for the rapid de novo folding of firefly luciferase. Nat. Struct. Biol. *6*, 697–705.

Gilon, T., Chomsky, O., and Kulka, R. G. (1998). Degradation signals for ubiquitin system proteolysis in *Saccharomyces cerevisiae*. EMBO J. *17*, 2759–2766.

Gregory, R. J., Rich, D. P., Cheng, S. H., Souza, D. W., Paul, S., Manavalan, P., Anderson, M. P., Welsh, M. J., and Smith, A. E. (1991). Maturation and function of CFTR variants bearing mutations in putative NBD1 and 2. Mol. Cell Biol. *11*, 3886–3893.

Han, J. H., Batey, S., Nickson, A. A., Teichmann, S. A., and Clarke, J. (2007). The folding and evolution of multidomain proteins. Nat. Rev. Mol. Cell Biol. *8*, 319–330.

He, L., Aleksandrov, A. A., Serohijos, A. W., Hegedus, T., Aleksandrov, L. A., Cui, L., Dokholyan, N. V., and Riordan, J. R. (2008). Multiple membrane-cytoplasmic domain contacts in cftr mediate regulation of channel gating. J. Biol. Chem. *283*, 26383–26390

Hegedus, T., Serohijos, A. W., Dokholyan, N. V., He, L., and Riordan, J. R. (2008). Computational studies reveal phosphorylation-dependent changes in the unstructured R domain of CFTR. J. Mol. Biol. *378*, 1052–1063.

Kartner, N., and Riordan, J. (1998). Characterization of polyclonal and monoclonal antibodies to cystic fibrosis transmembrane conductance regulator. Methods Enzymol. *292*, 629–652.

Klein-Seetharaman, J., Oikawa, M., Grimshaw, S. B., Wirmer, J., Duchardt, E., Ueda, T., Imoto, T., Smith, L. J., Dobson, C. M., and Schwalbe, H. (2002). Long-range interactions within a nonnative protein. Science *295*, 1719–1722.

Kleizen, B., van Vlijmen, T., de Jonge, H. R., and Braakman, I. (2005). Folding of CFTR is predominantly cotranslational. Mol. Cell *20*, 277–287.

Kopito, R. R. (1999). Biosynthesis and degradation of CFTR. Physiol. Rev. *79*, S167–S173.

Laney, J. D., and Hochstrasser, M. (1999). Substrate targeting in the ubiquitin system. Cell *97*, 427–430.

Lewis, H. A., *et al*. (2005). Impact of the deltaF508 mutation in first nucleotide-binding domain of human cystic fibrosis transmembrane conductance regulator on domain folding and structure. J. Biol. Chem. *280*, 1346–1353.

Lukacs, G. L., Mohamed, A., Kartner, N., Chang, X. B., Riordan, J. R., and Grinstein, S. (1994). Conformational maturation of CFTR but not its mutant counterpart (delta F508) occurs in the endoplasmic reticulum and requires ATP. EMBO J. *13*, 6076–6086.

Meacham, G., Patterson, C., Zhang, W., Younger, J., and Cyr, D. (2001). The Hsc70 co-chaperone CHIP targets immature CFTR for proteasomal degradation. Nat. Cell Biol. *3*, 100–105.

Meacham, G. C., Lu, Z., King, S., Sorscher, E., Tousson, A., and Cyr, D. M. (1999). The Hdj-2/Hsc 70 chaperone pair facilitates early steps in CFTR biogenesis. EMBO J. *18*, 1492–1505.

Mornon, J. P., Lehn, P., and Callebaut, I. (2008). Atomic model of human cystic fibrosis transmembrane conductance regulator: membrane-spanning domains and coupling interfaces. Cell Mol. Life Sci.

Nakatsukasa, K., and Brodsky, J. L. (2008). The recognition and retrotranslocation of misfolded proteins from the endoplasmic reticulum. Traffic *9*, 861–870.

Nicola, A., Chen, W., and Helenius, A. (1999). Co-translational folding of an alphavirus capsid protein in the cytosol of living cells. Nat. Cell Biol. *1*, 341–345.

Oberdorf, J., Pitonzo, D., and Skach, W. R. (2005). An energy-dependent maturation step is required for release of the cystic fibrosis transmembrane conductance regulator from early endoplasmic reticulum biosynthetic machinery. J. Biol. Chem. *280*, 38193–38202.

Ostedgaard, L., Baldursson, O., Vermeer, D., Welsh, M., and Robertson, A. (2000a). A functional R domain from cystic fibrosis transmembrane conductance regulator is predominantly unstructured in solution. Proc. Natl. Acad. Sci. USA *97*, 5657–5662.

Ostedgaard, L. S., Puldarsoon, O., Vomeer, D. V., Welsh, M. J., and Gittes, G. K. (2000b). A functional R domain from cystic fibrosis transmembrane conductance regulator is predominantly unstructured in solution. Proc. Natl. Acad. Sci. USA *97*, 5657–5662.

Owsianik, G., Cao, L., and Nilius, B. (2003). Rescue of functional DeltaF508-CFTR channels by co-expression with truncated CFTR constructs in COS-1 cells. FEBS Lett. *554*, 173–178.

Pagant, S., Brovman, E. Y., Halliday, J. J., and Miller, E. A. (2008). Mapping of interdomain interfaces required for the functional architecture of Yor1p, a eukaryotic ATP-binding cassette (ABC) transporter. J. Biol. Chem. *283*, 26444–26451.

Pakula, A. A., Young, V. B., and Sauer, R. T. (1986). Bacteriophage lambda cro mutations: effects on activity and intracellular degradation. Proc. Natl. Acad. Sci. USA *83*, 8829–8833.

Piguet, V., Gu, F., Foti, M., Demaurex, N., Gruenberg, J., Carpentirer, J., and Trono, D. (1999). Nef-induced CD4 degradation: a diacidic based motif in Nef functions as a lysosomal targeting signal trough the binding of β-COP in endosomes. Cell *97*, 63–73.

Riordan, J., Rommens, J., Kerem, B., Alon, N., Rozmahel, R., Grzelczak, Z., Zielenski, J., Lok, S., Plavsic, N., Chou, J., and et al. (1989). Identification of the cystic fibrosis gene: cloning and characterization of complementary DNA. Science *245*, 1066–1073.

Riordan, J. R. (2005). Assembly of functional CFTR chloride channels. Annu. Rev. Physiol. *67*, 701–718.

Riordan, J. R. (2008). CFTR function and prospects for therapy. Annu. Rev. Biochem. *77*, 701–726.

Rosser, M., Grove, D., Chen, L., and Cyr, D. (2008). Assembly and misassembly of CFTR: folding defects caused by deletion of F508 occur before and after the calnexin-dependent association of MSD1 and MSD2. Mol. Biol. Cell *19*, 4570–4579.

Roxo-Rosa, M., Xu, Z., Schmidt, A., Neto, M., Cai, Z., Soares, C. M., Sheppard, D. N., and Amaral, M. D. (2006). Revertant mutants G550E and 4RK rescue cystic fibrosis mutants in the first nucleotide-binding domain of CFTR by different mechanisms. Proc. Natl. Acad. Sci. USA *103*, 17891–17896.

Sadlish, H., and Skach, W. R. (2004). Biogenesis of CFTR and other polytopic membrane proteins: new roles for the ribosome-translocon complex. J. Membr. Biol. *202*, 115–126.

Seibert, F., Linsdell, P., Loo, T., Hanrahan, J., Clarke, D., and Riordan, J. (1996). Disease-associated mutations in the fourth cytoplasmic loop of cystic fibrosis transmembrane conductance regulator compromise biosynthetic processing and chloride channel activity. J. Biol. Chem. *271*, 15139–15145.

Serohijos, A. W., Hegedus, T., Aleksandrov, A. A., He, L., Cui, L., Dokholyan, N. V., and Riordan, J. R. (2008a). Phenylalanine-508 mediates a cytoplasmic-

membrane domain contact in the CFTR 3D structure crucial to assembly and channel function. Proc. Natl. Acad. Sci. USA *105*, 3256–3261.

Serohijos, A. W., Hegedus, T., Riordan, J. R., and Dokholyan, N. V. (2008b). Diminished self-chaperoning activity of the DeltaF508 mutant of CFTR results in protein misfolding. PLoS Comput. Biol. *4*, e1000008.

Sharma, M., *et al*. (2004). Misfolding diverts CFTR from recycling to degradation: quality control at early endosomes. J. Cell Biol. *164*, 923–933.

Sheppard, D., and Welsh, M. (1999). Structure and function of the CFTR chloride channel. Physiol. Rev. *79*, S23–S45.

Thibodeau, P. H., Brautigam, C. A., Machius, M., and Thomas, P. J. (2005). Side chain and backbone contributions of Phe508 to CFTR folding. Nat. Struct. Mol. Biol. *12*, 10–16.

Vashist, S., and Ng, D. T. (2004). Misfolded proteins are sorted by a sequential checkpoint mechanism of ER quality control. J. Cell Biol. *165*, 41–52.

Wang, W., Bernard, K., Li, G., and Kirk, K. L. (2007a). Curcumin opens cystic fibrosis transmembrane conductance regulator channels by a novel mechanism that requires neither ATP binding nor dimerization of the nucleotide-binding domains. J. Biol. Chem. *282*, 4533–4544.

Wang, X., Matteson, J., An, Y., Moyer, B., Yoo, J. S., Bannykh, S., Wilson, I. A., Riordan, J. R., and Balch, W. E. (2004). COPII-dependent export of cystic fibrosis transmembrane conductance regulator from the ER uses a di-acidic exit code. J. Cell Biol. *167*, 65–74.

Wang, X., *et al*. (2006). Hsp90 cochaperone Aha1 downregulation rescues misfolding of CFTR in cystic fibrosis. Cell *127*, 803–815.

Wang, Y., Loo, T. W., Bartlett, M. C., and Clarke, D. M. (2007b). Modulating the folding of P-glycoprotein and cystic fibrosis transmembrane conductance regulator truncation mutants with pharmacological chaperones. Mol. Pharmacol. *71*, 751–758.

Wenk, M., Jaenicke, R., and Mayr, E. M. (1998). Kinetic stabilisation of a modular protein by domain interactions. FEBS Lett. *438*, 127–130.

Winter, M., and Welsh, M. (1997). Stimulation of CFTR activity by its phosphorylated R domain. Nature *389*, 294–296.

Wiseman, R. L., Powers, E. T., Buxbaum, J. N., Kelly, J. W., and Balch, W. E. (2007). An adaptable standard for protein export from the endoplasmic reticulum. Cell *131*, 809–821.

Xiong, X., Bragin, A., Widdicombe, J. H., Cohn, J., and Skach, W. R. (1997). Structural cues involved in endoplasmic reticulum degradation of G85E and G91R mutant cystic fibrosis transmembrane conductance regulator. J. Clin. Invest. *100*, 1079–1088.

Youker, R. T., Walsh, P., Beilharz, T., Lithgow, T., and Brodsky, J. L. (2004). Distinct roles for the Hsp40 and Hsp90 molecular chaperones during cystic fibrosis transmembrane conductance regulator degradation in yeast. Mol. Biol. Cell *15*, 4787–4797.

Young, J. C., Agashe, V. R., Siegers, K., and Hartl, F. U. (2004). Pathways of chaperone-mediated protein folding in the cytosol. Nat. Rev. Mol. Cell Biol. *5*, 781–791.

Younger, J. M., Chen, L., Ren, H. Y., Rosser, M. F., Turnbull, E. L., Fan, C. Y., Patterson, C., and Cyr, D. M. (2006). Sequential quality-control checkpoints triage misfolded cystic fibrosis transmembrane conductance regulator. Cell *126*, 571–582.

Zerangue, N., Schwappach, B., Jan, Y. N., and Jan, L. Y. (1999). A new ER trafficking signal regulates the subunit stoichiometry of plasma membrane K(ATP) channels. Neuron *22*, 537–548.

Zhang, F., Kartner, N., and Lukacs, G. L. (1998). Limited proteolysis as a probe for arrested conformational maturation of ΔF508 CFTR. Nat. Struct. Biol. *5*, 180–183.

Zielenski, J., and Tsui, L.-C. (1995). Cystic fibrosis: genotypic and phenotypic variations. Annu. Rev. Genet. *29*, 777–807.